Anisotropic spin-flip-induced multiferroic behavior in kagome $Cu_3Bi(SeO_3)_2O_2Cl$

H. C. Wu,[1] K. Devi Chandrasekhar,[1] J. K. Yuan,[1] J. R. Huang,[2] J.-Y. Lin,[2] H. Berger,[3] and H. D. Yang[1]
[1]*Department of Physics, National Sun Yat-Sen University, Kaohsiung, 804 Taiwan*
[2]*Institute of Physics, National Chiao Tung University, Hsinchu 30010, Taiwan*
[3]*Institute of Physics of Complex Matter, Ecole Polytechnique Federal de Lausanne, CH-1015 Lausanne, Switzerland*
(Received 15 August 2016; revised manuscript received 2 February 2017; published 15 March 2017)

Compared to the previous report on $Cu_3Bi(SeO_3)_2O_2X$ ($X = Cl,Br$) [V. Gnezdilov *et al.*, (arXiv:1604.04249)],where no dielectric anomaly was observed without magnetic field near $T_N \sim 25.6$ K, we further present the dielectric behaviors without and with magnetic field in $Cu_3Bi(SeO_3)_2O_2Cl$. At zero field $H = 0$, an antiferromagnetic transition from magnetization and specific heat measurements is clearly established at T_N, while no dielectric anomaly was observed. Those results are similar to the previous report [V. Gnezdilov *et al.*, (arXiv:1604.04249)]. Above the critical field $H_c \sim 0.8$ T, a metamagnetic spin-flip transition from antiferromagnetic to ferrimagnetic order at $T \sim T_N$ is induced anisotropically only for $H \parallel c$. Meanwhile, a ferroelectric behavior from dielectric and pyroelectric current measurements is observed below $T \sim T_N$; then a corresponding type-II multiferroics emerges above H_c. The key mechanism of the anisotropic spin-flip-induced multiferroicity in $Cu_3Bi(SeO_3)_2O_2Cl$ can be ascribed to the breaking of magnetic twofold symmetry in the *bc* plane above H_c.

DOI: 10.1103/PhysRevB.95.125121

I. INTRODUCTION

Multiferroic materials have received a tremendous amount of research interest in the past decade because of their potential application in spin-based devices [1]. Physical insights into the coupling of the multiferroic property can be assigned to the correlation between the charge, spin, orbital, and lattice degrees of freedom [2]. To date, multiferroic behaviors have been demonstrated in a number of systems with the aid of theoretical calculations, along with the advancement of experimental techniques [3–7]. Several mechanisms such as the Dzyaloshinskii-Moriya (DM) interaction [3], exchange striction, geometric frustration [4,5], and metal-ligand hybridization (*p-d* interaction) [6,7] have been theoretically established to explain the multiferroic properties. Geometrical spin frustration systems such as triangular lattice, kagome lattice, pyrochlore lattice, and spinel structure play a major role in condensed matter to achieve diverse physical properties [8–12]. In addition to these frustrated materials, the mineral francisites of kagome $Cu_3Bi(SeO_3)_2O_2X$ ($X = Cl,Br$) possess the antiferromagnetic ordering temperature near 24 and 27.4 K and trigger a metamagnetic transition accompanied with a spin-flip behavior under the critical magnetic fields $H_c = 0.74$ T and 0.8 T parallel to the *c* axis [9,12]. More recently, Wang *et al.* [13] reported the magnetoelectric phase diagrams of multiferroic CuO using a high magnetic field up to 50 T, indicating that the magnetization, polarization, magnetocapacitance, and magnetostriction are closely related to the spin-flop phenomenon. Furthermore, there were only a few reports on field-induced electrical polarization such as hexaferrites [14], $DyFeO_3$ [15], and $NdCrTiO_5$ [16]. This motivates us to study the magnetodielectric coupling in $Cu_3Bi(SeO_3)_2O_2Cl$ in the presence of spin-flip behavior.

The mineral francisite $Cu_3Bi(SeO_3)_2O_2X$ ($X = Cl,Br$) possesses a complex, layered structure with Cu^{2+} spin 1/2 chains and crystallizes in an orthorhombic structure with the *Pmmn* space group [17]. It consists of two types of $[CuO_4]$ square plackets, sharing apices to form copper-oxygen layers reminiscent of a buckled kagome lattice [17]. Two Cu ions form an alternative chainlike structure in the *ab* plane. The Cu_1 chains are connected to Se^{4+} ions, whereas the Cu_2 chains contain selenium lone-pair electrons and chloride/bromide ions [17]. Besides the complex crystal structure, $Cu_3Bi(SeO_3)_2O_2X$ ($X = Cl,Br$) exhibits intriguing physical properties such as anisotropic magnetism. This property was explored in the dc magnetic studies below T_N [9,12]. When a critical magnetic field, $H_c \sim 0.8$ T, was applied perpendicular to the *ab* plane in $Cu_3Bi(SeO_3)_2O_2Br$, a metamagnetic transition jump from antiferromagnetic (AFM) to ferromagnetic (FM)/ferrimagneticlike (FIM) behavior was reported; every second layer flipped its spin orientation along the field direction [9,12]. Despite the lack of detailed studies of magnetic structure for $Cu_3Bi(SeO_3)_2O_2Cl$, similar magnetic features of $Cu_3Bi(SeO_3)_2O_2X$ ($X = Cl,Br$) were explored according to first-principles calculations, which suggest that the spin direction of the Cu_1 site deviates from the *c* axis with the *bc* angles $\theta = 50.1^\circ$ and 53.8° for $Cu_3Bi(SeO_3)_2O_2X$ ($X = Cl,Br$) [18]. More recently, based on Raman studies, $Cu_3Bi(SeO_3)_2O_2X$ ($X = Cl,Br$) was shown to present quantum magnetic fluctuations owing to the interplay of polar phonon modes [19]. In addition, only $Cu_3Bi(SeO_3)_2O_2Cl$ undergoes a second-order structural phase and its structure becomes polar with ferroelectricity [19]. However, $Cu_3Bi(SeO_3)_2O_2Cl$ was investigated for antiferroelectric distortion below 115 K with nonpolar *Pcmn* symmetry using low-temperature synchrotron powder diffraction, while $Cu_3Bi(SeO_3)_2O_2Br$ does not exhibit low-temperature structural transformation down to 10 K [20]. In this article, magnetodielectric and pyroelectric measurements were further conducted to study the coupling between magnetism and electricity and the possible multiferroic behavior in $Cu_3Bi(SeO_3)_2O_2Cl$ single crystals.

II. EXPERIMENTAL METHODS

Single crystals of $Cu_3Bi(SeO_3)_2O_2Cl$ were grown using the chemical vapor-phase method and the detailed synthesis

process is described in Ref. [9]. The typical crystal thickness was 2 mm with the crystal orientated with the c axis along the surface normal. The measurements of dc magnetization (M) and ac susceptibility (χ'_{ac}) with respect to the field (H) and temperature (T) were performed using a Quantum Design MPMS system (MPMS-XL 7). The low-temperature heat capacity C (T, H) was collected with a ^{3}He heat-pulsed thermal relaxation calorimeter. The platelike $Cu_3Bi(SeO_3)_2O_2Cl$ single crystal was coated with silver paint as the electrodes ($E \parallel c$). The dielectric permittivity was obtained using commercial systems (MPMS-XL 7 and PPMS Quantum design 6200) with home-made capacitance probes and was collected using an Agilent 4294A precision impedance analyzer with an ac excitation voltage of 1 V. A maximum field of 5 T was employed during the temperature- and field-dependent dielectric measurements. The electrical polarization was obtained from the pyrocurrent data. A 300 V electrical poling was applied during the cooling process, and the pyrocurrent was collected using a Keithley 6517 B electrometer. Temperature-dependent synchrotron x-ray patterns were taken by the Taiwan Photon Source (TPS) 09A beamline with a step of angle 0.004° in the National Synchrotron Radiation Research Center (NSRRC), Hsinchu, Taiwan.

III. RESULTS AND DISCUSSION

A. Dc magnetization

Figure 1(a) displays the M-T curves of single-crystal $Cu_3Bi(SeO_3)_2O_2Cl$ with an external magnetic field (100 Oe) applied along the directions parallel ($H \parallel c$) and perpendicular to the c axis ($H \perp c$). Both curves display a sharp maximum at 25.6 K, indicating a paramagnetic (PM) to antiferromagnetic (AFM) transition. The M-H curves of $Cu_3Bi(SeO_3)_2O_2Cl$ at 5 K for $H \parallel c$ and $H \perp c$ are shown in the inset of Fig. 1(a). The linear variation of the M-H curve for the $H \perp c$ orientation demonstrates strong AFM behavior. However, for the $H \parallel c$ orientation, an abrupt metamagnetic jump occurs at critical field $H_c \sim 0.8$ T, and a near-saturation behavior is thereafter noticed and can be ascribed to a spin-flip transition under a critical magnetic field. To further explore the spin-flip phenomena, temperature-dependent magnetization measurements were performed for the $H \parallel c$ orientation under different magnetic fields shown in Fig. 1(b). For $H = 0.01$ and 0.5 T, the magnetic properties exhibit AFM behavior with T_N shifts towards lower temperatures as increasing H. For $H = 1$ and 2 T, the magnetization curves indicate saturation as $T < T_N$, demonstrating the spin-flip and FM/FIM-like behavior. The field-induced metamagnetic transitions recorded at different temperatures are shown in the inset of Fig. 1(b). It can be observed that the critical field for the field-induced spin-flip behavior decreases with increasing temperature. These results are consistent and similar to those reported in some studies [9,12]. Above T_N, the spin flip entirely disappears and a linear M-H curve at 35 K exhibits PM behavior.

B. Ac susceptibility and specific heat

To elucidate the nature of the phase transition below and above H_c, temperature-dependent ac susceptibility (χ'_{ac}) and specific heat (C) measurements of $Cu_3Bi(SeO_3)_2O_2Cl$ were

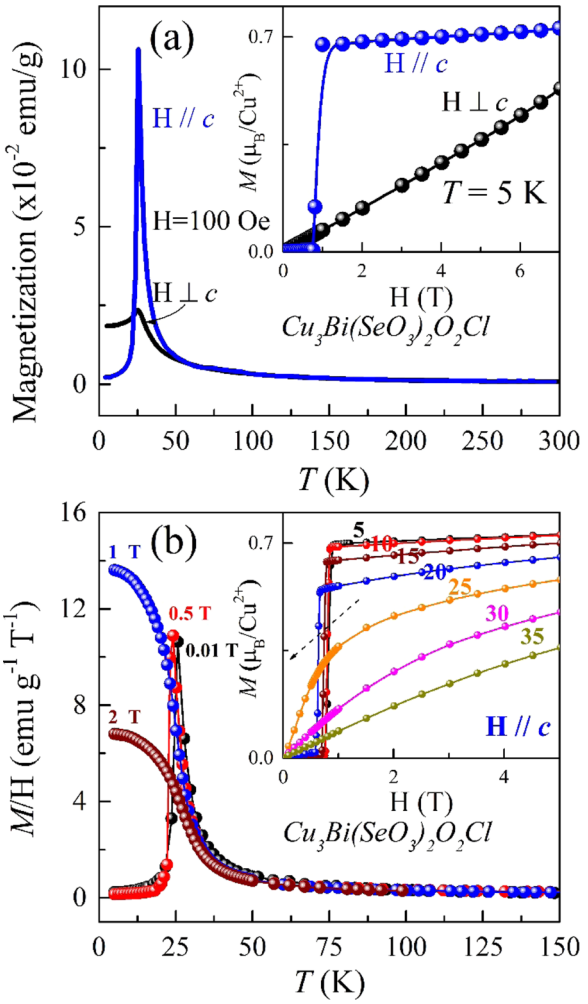

FIG. 1. (a) Temperature-dependent magnetization of single-crystal $Cu_3Bi(SeO_3)_2O_2Cl$ with the application of a magnetic field of 100 Oe for $H \parallel c$ and $H \perp c$. The inset shows the isothermal M-H curve of $Cu_3Bi(SeO_3)_2O_2Cl$ at 5 K with an applied magnetic field up to 5 T for $H \parallel c$ and $H \perp c$. (b) Temperature-dependent magnetization of single-crystal $Cu_3Bi(SeO_3)_2O_2Cl$ with different magnetic fields for $H \parallel c$. The inset shows M-H curves at several temperatures with $H \parallel c$.

performed for $H \parallel c$. The results are presented in Figs. 2(a) and 2(b). In the zero-magnetic field, a frequency-independent [inset in Fig. 2(a)] sharp peak in χ'_{ac} vs T is observed. Furthermore, a pronounced λ-type anomaly in C/T vs T signifies a long-range order below 26 K. For $H > H_c$, the field-induced metamagnetic transition suddenly diminishes the sharp anomalies in χ'_{ac}. The absence of thermal hysteresis in C/T (data not shown) suggests a second-order phase transition with respect to T. For $H = 0.5$ T, the peak is slightly shifted to a lower temperature in both χ'_{ac} vs T and C/T vs T curves, as expected for an AFM order. Indeed, a smeared peak in χ'_{ac} is observed and shifted to a higher temperature with an increase in H. As for C/T, the pronounced peak suddenly becomes a broad anomaly at $H > H_c$. This broad feature also shifts to higher T with increasing H. In actuality, the above-described evolution of C/T in H is similar to that in MnSi skyrmions, where the high-field regime is a

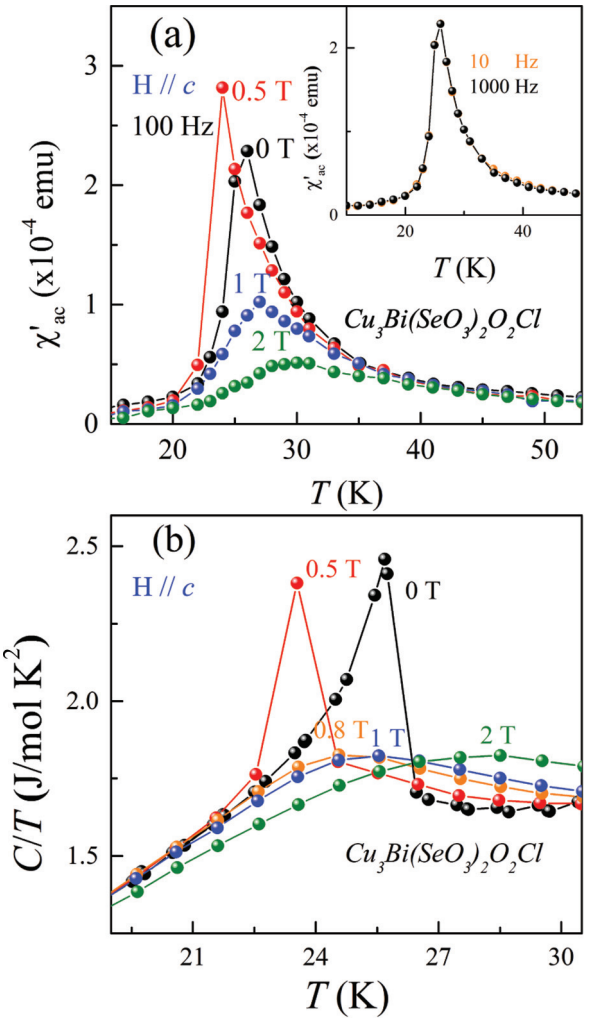

FIG. 2. (a) Temperature-dependent ac susceptibility (χ'_{ac}) of $Cu_3Bi(SeO_3)_2O_2Cl$ with the application of dc magnetic fields 0, 0.5, 1, and 2 T for $H \parallel c$. The inset shows χ'_{ac}-T of $Cu_3Bi(SeO_3)_2O_2Cl$ at a frequency of 10 and 1000 Hz. (b) Temperature-dependent specific heat (C) of single-crystal $Cu_3Bi(SeO_3)_2O_2Cl$ with magnetic fields 0, 0.5, 0.8, 1, and 2 T for $H \parallel c$.

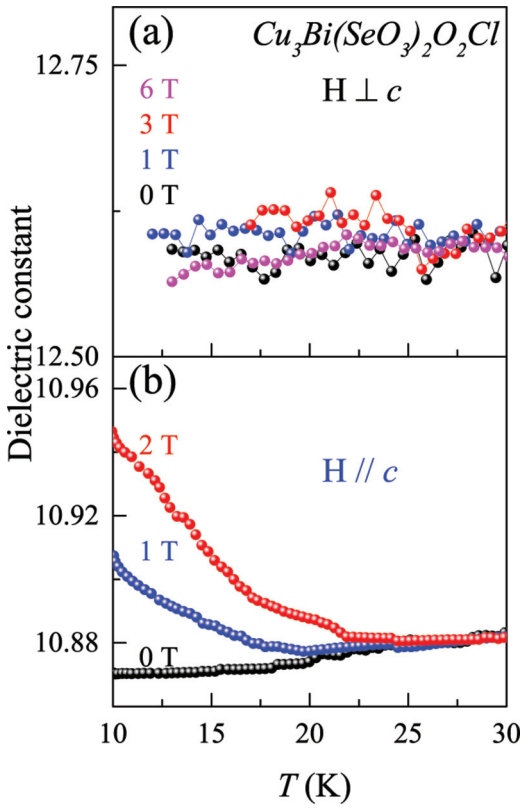

FIG. 3. Temperature-dependent dielectric constant measurements of single-crystal $Cu_3Bi(SeO_3)_2O_2Cl$ with the application of different magnetic fields for (a) $H \perp c$ and (b) $H \parallel c$.

field-polarized one [21]. Moreover, the broad feature above H_c indicates a crossover line between the paramagnetic phase and field-polarized (or ferrimagnetic) regime. There have been several other metamagnetic systems such as $Pr_{0.63}Ca_{0.37}MnO_3$, Y_2CoMnO_6, and $(Eu_{0.4}La_{0.1})(Sr_{0.4}Ca_{0.1})MnO_3$, where the field-forced AFM order to FM- or FIM-like phase is ascribed to the first-order phase transition [22–24]. The present case of $Cu_3Bi(SeO_3)_2O_2Cl$ is likely reminiscent of some of them.

C. Dielectric, magnetodielectric, and pyrocurrent measurements

To observe the anisotropic effects on the magnetodielectric property, temperature-dependent dielectric measurements were performed using several magnetic fields with both $H \perp c$ and $H \parallel c$ orientations. As illustrated in Fig. 3(a), the dielectric permittivity for the $H \perp c$ orientation does not exhibit an anomaly near T_N with the magnetic field region between 0 and 6 T. However, there is a significant enhancement in the low-temperature dielectric permittivity for the $H \parallel c$ orientation when $H = 1$ and 2 T, as indicated in Fig. 3(b). The anisotropic dielectric behavior is very similar to the magnetization behavior, suggesting that the metamagnetic spin-flip transition triggers a large anisotropic magnetodielectric on the system.

Furthermore, the field-dependent dielectric and polarization measurements for $H \parallel c$ at 10 K were performed to explore the coupling between magnetism and electricity in $Cu_3Bi(SeO_3)_2O_2Cl$. The spin flip at H_c induces a step jump in the M-H curve [Fig. 4(a)]. From the schematic diagram shown in Fig. 7, the Cu_1 and Cu_2 spins at alternative layers exhibit a flip for $H \parallel c$, which leads to an abrupt jump in magnetization. However, as $H_c \sim 0.8$ T, the magnetization reaches $0.68\,\mu_B/Cu^{2+}$, which is smaller than the expected magnetization of $1\,\mu_B/Cu^{2+}$, indicating that the spin-flip transition does indeed alter the magnetic state from AFM to FIM ordering. When $H > H_c$, the magnetization exhibits a slow variation because of the field-forced alignment of FIM. Figure 4(b) displays the field-dependent dielectric property for $H \parallel c$. As $H < H_c$, the dielectric permittivity is insensitive to the field variation. However, as $H_c \sim 0.8$ T, an abrupt drop in dielectric property is noticed, reminiscent of the magnetization jump, suggesting that the spin flip plays an important role in the observed variations. Furthermore, the field-dependent electrical polarization also exhibits a finite peak near the H_c value, as shown in Fig. 4(c), indicating that the spin flip triggers a ferroelectric property in $Cu_3Bi(SeO_3)_2O_2Cl$. In other words,

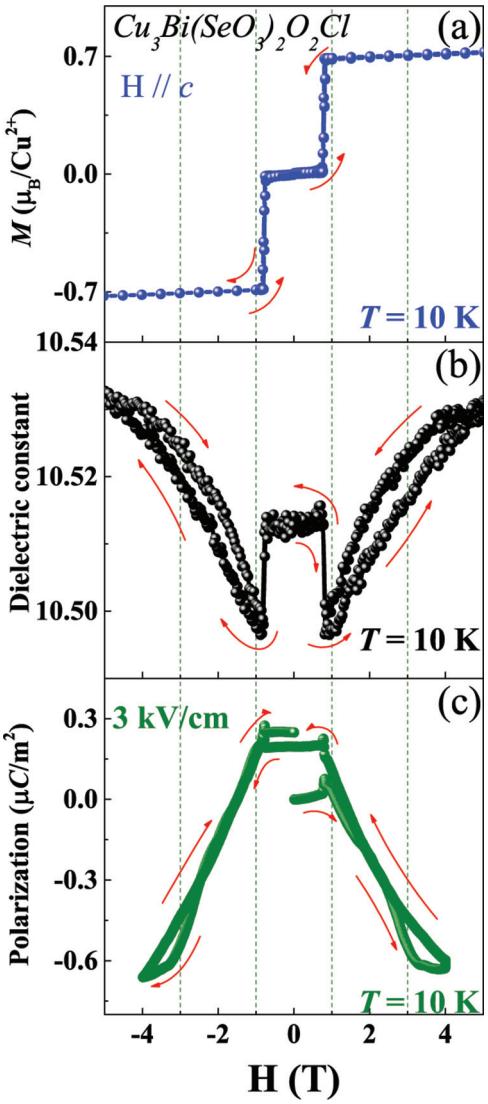

FIG. 4. (a) Isothermal magnetic hysteresis loop, (b) field-dependent dielectric constant, and (c) polarization measurement of single-crystal $Cu_3Bi(SeO_3)_2O_2Cl$ for $H \parallel c$ at 10 K. Red arrows indicate the measuring cycling process.

the magnetic field induces type-II multiferroic behavior with the coexistence of ferrimagneticism and ferroelectricity at $T < 25$ K and $H \geqslant 0.8$ T. In contrast to magnetization, dielectric permittivity and polarization display a finite hysteresis with the field variation above H_c. This difference might be related to the high inertia of electric dipoles compared to magnetic spins, indicating that electric dipoles could be more difficulty to controlled than magnetic spins. A similar kind of type-II multiferroic behavior was noticed in the orthorhombic $DyFeO_3$ system along the $H \parallel c$ orientation [15]. The field-forced spin reorientation of Fe moments below Dy ordering creates an exchange striction between the Dy and Fe layers, leading to ferroelectric ordering for $T = 3$ K and $H_c \geqslant 2.4$ T [15]. However, in the present case, the type-II multiferroic occurs at a much higher temperature ($T < 25$ K) and lower field ($H_c \geqslant 0.8$ T) than in the case of $DyFeO_3$ [15].

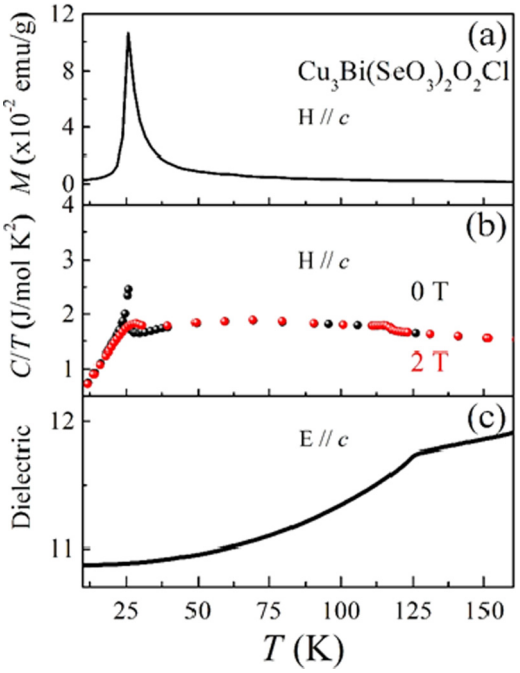

FIG. 5. Temperature-dependent (a) magnetization, (b) specific heat, and (c) dielectric constant measurements of $Cu_3Bi(SeO_3)_2O_2Cl$ single crystal for $H \parallel c$ and $E \parallel$ c.

D. High-temperature phase transitions

The room temperature X-ray diffraction (XRD) pattern of $Cu_3Bi(SeO_3)_2O_2Cl$ displays orthorhombic structure with the space group *Pmmn* ($a = 6.3502$ (2) Å, $b = 9.6280$ (3) Å and $c = 7.2280$ (2) Å) [25]. Gnezdilov *et al.* [19] confirmed the change of crystal structure in $Cu_3Bi(SeO_3)_2O_2Cl$ from centrosymmetric to noncentrosymmetric around 120 K through Raman studies. Thus further dielectric and specific anomalies at 120 K support the appearance of electric dipoles in $Cu_3Bi(SeO_3)_2O_2Cl$. In fact, similar anomalies were also observed in dielectric permittivity and specific heat data near 117 K (shown in Fig. 5). However, pyroelectric measurements (I_p) in $Cu_3Bi(SeO_3)_2O_2Cl$ were performed, signifying the absence of spontaneous electrical polarization at 120 K. In addition, further detailed structural studies of $Cu_3Bi(SeO_3)_2O_2Cl$ were collected by the Taiwan Photon Source (TPS) 09A beamline with a step of angle 0.004° to explore whether it shows structural change or not (shown in Fig. 6). At 80 K, a new Bragg reflection peak appears and could be indexed as a 301 peak with *Pcmn* space group, indicating that $Cu_3Bi(SeO_3)_2O_2Cl$ undergoes a structural change from nonpolar *Pmmn* to nonpolar *Pcmn* below 120 K. Here, we could eliminate the possibility of polar $P2_1mn$ structure and ferroelectricity in $Cu_3Bi(SeO_3)_2O_2Cl$ below 120 K. This result is in agreement with a recent report [20] which presents antiferroelectric distortion using density-functional calculations of lattice dynamics and high-resolution synchrotron powder diffraction in $Cu_3Bi(SeO_3)_2O_2Cl$. At this moment, we can only suggest two possibilities: (i) At a macroscopic level, the spontaneous polarization from electrical dipoles is very low; or (ii) $Cu_3Bi(SeO_3)_2O_2Cl$ could be an antiferroelectric material with no net polarization.

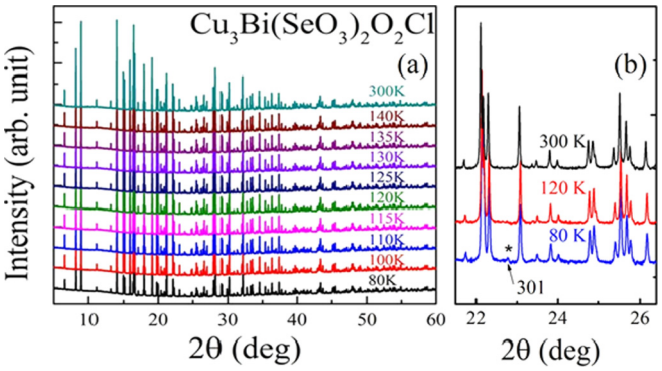

FIG. 6. (a) Synchrotron powder XRD of $Cu_3Bi(SeO_3)_2O_2Cl$ at selected temperatures from 80 to 300 K. (b) The new Bragg reflection peak of 301 appears at 80 K.

Because of the coexistence of FIM and FE ordering in $Cu_3Bi(SeO_3)_2O_2Cl$ as $H > H_c$ and $T < T_N$, its multiferroic nature is now demonstrated. The magnetic properties of $Cu_3Bi(SeO_3)_2O_2Cl$ indicate a strong anisotropy below T_N. This anisotropy stems from the microscopic details of the magnetic structure. $Cu_3Bi(SeO_3)_2O_2Cl$ has a layered crystal

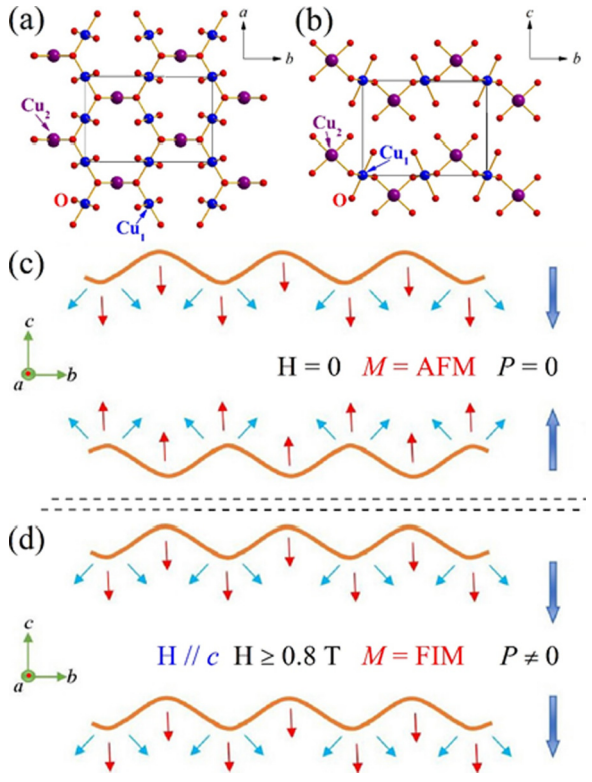

FIG. 7. The orthorhombic crystal structure with the space group *Pmmn*. The small (blue), large (purple), and small (red) balls indicate the Cu_1, Cu_2, and O atoms, respectively for (a) *ab* plane and (b) *bc* plane. Schematic diagram of layered spin structure, which is taken from Ref. [12] in a *bc* plane for $Cu_3Bi(SeO_3)_2O_2Cl$ for (c) $H = 0$ and (d) $H \geqslant 0.8$ T. Blue and red arrows of each layer represent Cu_1 and Cu_2 spins, respectively. The solid orange curve indicates the spin structure within each layer. Large blue arrows denote the expected polarization direction of each layer.

structure with complex magnetic interactions. The two Cu_1O_4 and Cu_2O_4 sites, respectively, occupy two different crystallographic positions in the *ab* plane; these form two-dimensional (2D) magnetic layers [17]. Cu_1 and Cu_2 ions are connected to each other similar to a pseudo-kagome lattice in the *ab* plane. The Cu_1-O_1-Cu_1 and Cu_1-O_1-Cu_2 bonds almost have similar bond lengths and angles that exhibit superexchange FM behavior [12]. The former magnetic interaction is backed by an additional exchange path via a lone-pair Bi^{3+} ion, i.e., Cu_1-O_1-Bi-O_1-Cu_1. This magnetic interaction along with the magnetic frustrations by the kagome geometry creates a sizable AFM interaction between the Cu_1-Cu_1 ions. The competing FM and AFM interactions form an unconventional FIM state, where spins arrange in a canting configuration with the magnetic moments oriented 50° from *c* towards *b* [12]. However, the spin of Cu_2 is oriented strictly parallel to the *c* axis with an antiparallel alignment between the layers along the *c* axis. The spin structure in the *bc* plane exhibits a twofold rotation symmetry. From neutron diffraction studies, when $H \perp ab$, the first-order-like metamagnetic spin-flip nature for the critical field of 0.8 T emerges [12]. Similar field-induced phenomena in the dielectric and FE behaviors (Fig. 4) might indicate the origin of the multiferroic nature hidden in the same single magnetic building block [26]. The canted ferrimagnetic magnetic structure in the *ab* plane is represented in the schematic diagram of Fig. 7. Spin moments within each layer form the spin structure; they are denoted by solid orange lines in Fig. 7. The spin structure is out of phase between the layers. Spin canting within each layer produces a finite DM interaction vector that creates the electric polarization parallel to the spin moment, denoted by large blue arrows in Fig. 7. In the low-magnetic field ($H < 0.8$ T), the twofold symmetry of the magnetic structure creates a net zero electric polarization due to the cancellation between the *ab* layers. However, for $H > H_c$, the field-induced spin flip breaks the twofold symmetry and generates a nonzero electric polarization along the *c* axis as illustrated in Fig. 7. Recent theoretical studies by Rousochatzakis *et al.* suggested that the dominating DM vector along the Cu_1-O_1-Cu_2 bond is crucial in determining

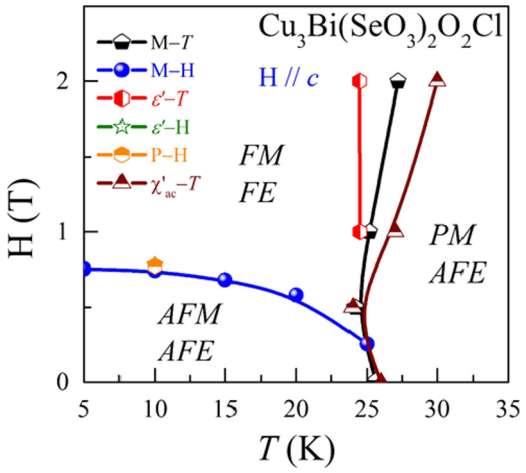

FIG. 8. The *H*-*T* phase diagram of single-crystal $Cu_3Bi(SeO_3)_2O_2Cl$ is determined by magnetization, ac susceptibility, dielectric constant, and pyroelectric current measurements.

the microscopic details of the magnetic structure, i.e., Cu_1 spin canting and anisotropic magnetic properties [27]. In addition, for the lower-temperature part, the H-T phase diagram of single-crystal $Cu_3Bi(SeO_3)_2O_2Cl$ shown in Fig. 8 could be plotted using magnetization, ac susceptibility, dielectric constant, and pyroelectric current measurements.

IV. CONCLUSION

A unique type-II multiferroic system in kagome $Cu_3Bi(SeO_3)_2O_2Cl$ at $T < 25\,\mathrm{K}$ and $H \geqslant 0.8\,\mathrm{T}$ is established with a magnetic field-induced coexistence of ferrimagnetism and ferroelectricity. The magnetic-field-dependent magnetization measurements and magnetodielectric effects of $Cu_3Bi(SeO_3)_2O_2Cl$ demonstrate a strong anisotropic behavior. The spin-flip-induced ferroelectricity was confirmed from the magnetic-field-dependent dielectric constant and electric polarization. The mechanism of field-induced multiferroic phenomena in $Cu_3Bi(SeO_3)_2O_2Cl$ could be related to the breaking of twofold symmetry of the magnetic blocks. These findings provide an interesting insight into the multiferroics in spin-flip metamagnetic materials.

ACKNOWLEDGMENTS

This work was supported by the Ministry of Science and Technology, Taiwan, under Grant No. MOST: 103-2112-M-110-010-MY3.

[1] S.-W. Cheong and M. Mostovoy, Nat. Mater. **6**, 13 (2007).
[2] W. Eerenstein, N. D. Mathur, and J. F. Scott, Nature **442**, 759 (2006).
[3] T. Kimura, T. Goto, H. Shintani, K. Ishizaka, T. Arima, and Y. Tokura, Nature **426**, 55 (2003).
[4] M. Pregelj, A. Zorko, O. Zaharko, P. Jeglič, Z. Kutnjak, Z. Jagličić, S. Jazbec, H. Luetkens, A. D. Hillier, H. Berger, and D. Arčon, Phys. Rev. B **88**, 224421 (2013).
[5] T. Besara, E. S. Choi, K. Y. Choi, P. L. Kuhns, A. P. Reyes, P. Lemmens, H. Berger, and N. S. Dalal, Phys. Rev. B **90**, 054418 (2014).
[6] H. Murakawa, Y. Onose, S. Miyahara, N. Furukawa, and Y. Tokura, Phys. Rev. Lett. **105**, 137202 (2010).
[7] K. Yamauchi, P. Barone, and S. Picozzi, Phys. Rev. B **84**, 054440 (2011).
[8] S. Nakatsuji, Y. Machida, Y. Maeno, T. Tayama, T. Sakakibara, J. van Duijn, L. Balicas, J. N. Millican, R. T. Macaluso, and J. Y. Chan, Phys. Rev. Lett. **96**, 087204 (2006).
[9] K. H. Miller, P. W. Stephens, C. Martin, E. Constable, R. A. Lewis, H. Berger, G. L. Carr, and D. B. Tanner, Phys. Rev. B **86**, 174104 (2012).
[10] S. T. Bramwell and M. J. P. Gingras, Science **294**, 1495 (2001).
[11] C. P. Sun, C. C. Lin, J. L. Her, C. J. Ho, S. Taran, H. Berger, B. K. Chaudhuri, and H. D. Yang, Phys. Rev. B **79**, 214116 (2009).
[12] M. Pregelj, O. Zaharko, A. Günther, A. Loidl, V. Tsurkan, and S. Guerrero, Phys. Rev. B **86**, 144409 (2012).
[13] Z. Wang, N. Qureshi, S. Yasin, A. Mukhin, E. Ressouche, S. Zherlitsyn, Y. Skourski, J. Geshev, V. Ivanov, M. Gospodinov, and V. Skumryev, Nat. Commun. **7**, 10295 (2016).
[14] S. H. Chun, Y. S. Chai, B.-G. Jeon, H. J. Kim, Y. S. Oh, I. Kim, H. Kim, B. J. Jeon, S. Y. Haam, J.-Y. Park, S. H. Lee, J.-H. Chung, J.-H. Park, and K. H. Kim, Phys. Rev. Lett. **108**, 177201 (2012).
[15] Y. Tokunaga, S. Iguchi, T. Arima, and Y. Tokura, Phys. Rev. Lett. **101**, 097205 (2008).
[16] J. Hwang, E. S. Choi, H. D. Zhou, J. Lu, and P. Schlottmann, Phys. Rev. B **85**, 024415 (2012).
[17] P. Millet, B. Bastide, V. Pashchenko, S. Gnatchenko, V. Gapon, Y. Ksarid, and A. Stepanovd, J. Mater. Chem. **11**, 1152 (2001).
[18] S. A. Nikolaev, V. V. Mazurenko, A. A. Tsirlin, and V. G. Mazurenko, Phys. Rev. B **94**, 144412 (2016).
[19] V. Gnezdilov, Yu. Pashkevich, V. Kurnosov, P. Lemmens, E. Kuznetsova, P. Berdonosov, V. Dolgikh, K. Zakharov, and A. Vasiliev, arXiv:1604.04249.
[20] D. A. Prishchenko, A. A. Tsirlin, V. Tsurkan, A. Loidl, A. Jesche, and V. G. Mazurenko, Phys. Rev. B **95**, 064102 (2017).
[21] A. Bauer, M. Garst, and C. Pfleiderer, Phys. Rev. Lett. **110**, 177207 (2013).
[22] V. Hardy, A. Wahl, C. Martin, and Ch. Simon, Phys. Rev. B **63**, 224403 (2001).
[23] J. Krishna Murthy, K. D. Chandrasekhar, H. C. Wu, H. D. Yang, J. Y. Lin, and A. Venimadhav, Europhys. Lett. **108**, 27013 (2014).
[24] D. S. Rana and S. K. Malik, Phys. Rev. B **74**, 052407 (2006).
[25] See Supplemental Material at http://link.aps.org/supplemental/10.1103/PhysRevB.95.125121 for a description of XRD characterization.
[26] Y. Wang, G. L. Pascut, B. G. T. A. Tyson, K. Haule, V. Kiryukhin, and S.-W. Cheong, Sci. Rep. **5**, 12268 (2015).
[27] I. Rousochatzakis, J. Richter, R. Zinke, and A. A. Tsirlin, Phys. Rev. B **91**, 024416 (2015).